Disulfide Bond Structure and Domain Organization of Yeast β(1,3)-Glucanosyltransferases Involved in Cell Wall Biogenesis*[s]

Laura Popolo[‡1], Enrico Ragni[‡2], Cristina Carotti[‡], Oscar Palomares[§], Ronald Aardema[¶], Jaap Willem Back[¶], Henk L. Dekker[¶], Leo J. de Koning[¶], Luitzen de Jong[¶], and Chris G. de Koster[¶]

From the ‡Dipartimento di Scienze Biomolecolari e Biotecnologie, Università degli Studi di Milano, 20133 Milano, Italy, the §Departamento de Bioquimica y Biologia Molecular, Facultad de Ciencias Quimicas, Universidad Complutense, 28040 Madrid, Spain, and ¶Biomolecular Mass Spectrometry Group, Swammerdam Institute for Life Sciences, University of Amsterdam, Nieuwe Achtergracht 166, 1018 WV Amsterdam, The Netherlands

The Gel/Gas/Phr family of fungal β(1,3)-glucanosyltransferases plays an important role in cell wall biogenesis by processing the main component β(1,3)-glucan. Two subfamilies are distinguished depending on the presence or absence of a C-terminal cysteine-rich domain, denoted "Cys-box." The N-terminal domain (NtD) contains the catalytic residues for transglycosidase activity and is separated from the Cys-box by a linker region. To obtain a better understanding of the structure and function of the Cys-box-containing subfamily, we identified the disulfide bonds in Gas2p from *Saccharomyces cerevisiae* by an improved mass spectrometric methodology. We mapped two separate intra-domain clusters of three and four disulfide bridges. One of the bonds in the first cluster connects a central Cys residue of the NtD with a single conserved Cys residue in the linker. Site-directed mutagenesis of the Cys residue in the linker resulted in an endoplasmic reticulum precursor that was not matured and underwent a gradual degradation. The relevant disulfide bond has a crucial role in folding as it may stabilize the NtD and facilitate its interaction with the C-terminal portion of a Gas protein. The four disulfide bonds in the Cys-box are arranged in a manner consistent with a partial structural resemblance with the plant X8 domain, an independent carbohydrate-binding module that possesses only three disulfide bonds. Deletion of the Cys-box in Gas2 or Gas1 proteins led to the formation of an NtD devoid of any enzymatic activity. The results suggest that the Cys-box is required for proper folding of the NtD and/or substrate binding.

In yeast and fungal cells, the cell wall determines cell shape, protects cells from lysis, and constitutes a permeability barrier to the uptake of exogenous substances. In fungal pathogens, the cell wall is also the interface for interactions with the host and is required for cell adhesion and virulence. In yeast, the extracellular matrix is formed and strengthened by the correct cross-linking of several polymers, mannoproteins, glucans, and chitin (1, 2) where β(1,3)-glucan is the most abundant polymer forming a helical, branched structure that is probably responsible for the elastic properties of the cell wall (3, 4). A plasma membrane β(1,3)-glucan synthase complex extrudes the polymer outside the cell, and other families of enzymes are responsible for its incorporation into the cell wall and for the anchoring of the other components in a way that is still poorly understood (1). The Gel/Gas/Phr family of proteins plays an essential role in cell wall biogenesis acting as β(1,3)-glucan processing enzymes (5, 6). *In vitro* these proteins catalyze a β(1,3)-glucanosyltransferase reaction that consists of the cleavage of an internal glycosidic linkage of a β(1,3)-glucan chain, the release of the reducing portion, and the transfer of the new reducing end to the nonreducing end of another acceptor β(1,3)-glucan (5, 6). Thus β(1,3)-glucanosyltransferases act similarly to glycoside hydrolases, but a carbohydrate functions as the acceptor rather than a water molecule (5). This preference for transglycosylation rather than hydrolysis presumably reflects structural differences between β(1,3)-glucanosyltransferases and β(1,3)-glucanases.

Proteins related to the Gel/Gas/Phr family are present in many yeast and fungal species and form family GH72 of glycoside hydrolases. GH72 enzymes are crucial for proper morphogenesis. Mutants deleted for the *GAS1* gene in *Saccharomyces cerevisiae* display morphological defects and reduced growth (7) and counteract lysis by activating a compensatory response involving the up-regulation of several genes (7–12). Mutants null for *GAS2* and *GAS4* produce inviable spores because of severe spore wall defects and the same phenotype is exhibited by mutants of *Schizosaccharomyces pombe* deleted for *GAS4* (13, 14). In *Aspergillus fumigatus* and *Candida albicans*, strains carrying mutations in the homologs of these genes, belonging to *GEL* and *PHR* gene families, show a great reduction in virulence in animal models of infection (15, 16). Because of the importance of this class of proteins in cell wall construction and virulence, they are promising molecular targets for new antifungal drugs.

Sequence analysis showed that members of GH72 family share a putative catalytic domain and a linker segment in the N-terminal region but differ significantly in the C-terminal

portion where a cysteine-enriched module (Cys-box) and a polyserine region of variable length (Ser-box) may be present in different arrangements (17). In a previous work (17), we described the identification of two distinct GH72 subfamilies based on the presence (GH72^{+}) or absence of the Cys-box (GH72^{−}). In addition all GH72 proteins share a glycosylphosphatidylinositol (GPI)[3] attachment signal at the C-terminal end. The GPI anchor tethers these proteins to the plasma membrane, but at least some members, *e.g.* Gas1p, Gas3p, and Gas5p of *S. cerevisiae*, are further processed and become covalently cross-linked to the cell wall via a glycosidic bond between a GPI remnant and $\beta(1,3)$-glucan-linked $\beta(1,6)$-glucans (18, 19).

The organization of domains of GH72^{+} proteins resembles that of many polysaccharide-hydrolyzing enzymes such as mannanases, chitinases, cellulases, and glucanases that are composed of the following distinct domains: a putative catalytic module and a noncatalytic module connected by a flexible region (20, 21). The noncatalytic module is often an independent appendix required for tight polysaccharide binding, and it is necessary for targeting secreted enzymes to the sites where hydrolysis takes place and for increasing the local concentration of the enzyme or in some cases for disrupting the fibrillar structure of the substrate (as for example in cellulose binding domains (20, 21).

In this work we have analyzed the disulfide bond structure and domain organization of Gas1p and Gas2p, two GH72^{+} enzymes of *S. cerevisiae*. We have mapped seven disulfide bonds in Gas2p by a recently developed computer-assisted mass spectrometric approach (22). Results suggest that the Cysbox tightly interacts with the NtD. Truncation analyses reveal a unique domain organization of Gas1 and Gas2 proteins as well as a role for the Linker region and a crucial Cys residue in the attainment of the properly folded and active conformation of the enzyme.

EXPERIMENTAL PROCEDURES

General Strategy Used to Identify Disulfide-linked Peptides—Our analytical strategy of the protein under study consists of cleavage between adjacent Cys residues and mass spectrometric analysis of the peptide mixture (see supplemental Fig. S1 for a flow chart). Free –SH groups were first alkylated under conditions preventing disulfide exchange reactions. Cleavage was accomplished by partial hydrolysis at low pH at Asp residues, combined with digestion by endoproteinase Glu-C. Peptides were separated by reversed-phase liquid chromatography (LC) directly coupled to electrospray ionization and Fourier transform ion cyclotron resonance (FTICR) mass spectrometry to provide the high mass accuracy required for unambiguous nomination of candidate disulfide-linked peptides (given the

large number of theoretical disulfide-linked combinations that exists with the chosen cleavage steps from a protein as complicated as Gas2p (22)). To identify linear peptides for internal calibration of the FTICR mass spectrometer, the peptide sample is first subjected to LC and tandem mass spectrometry (LC/MS/MS) on a quadrupole time-of-flight mass spectrometer. The MS/MS data are also used to validate the structures of candidate disulfide-linked peptides as revealed by accurate mass measurement. Disulfide linkages in peptides with two disulfide bonds are identified by mass spectrometry after partial reduction of disulfide bonds, cyanylation of Cys residues, and peptide bond cleavage at cyanylated residues.

Alkylation and Digestion—One part of a solution containing 1.2 M iodoacetamide, 6 M guanidinium HCl, and 10 mM sodium acetate, pH 4.0, was added to 4 parts of a solution containing 0.75 mg/ml sGas2p, 6 M guanidinium chloride, and 10 mM sodium acetate, pH 4.0. The pH was raised to 8 by addition of a solution of 1.2 M ammonium bicarbonate in 6 M guanidinium HCl to obtain a final concentration of 0.2 M ammonium bicarbonate. After incubation for 15 min at room temperature, the reaction mixture was dialyzed against water in six washes at 6 °C using an Ultrafree-0.5 centrifugal filter-type device Biomax-10 (Millipore, Bedford, MA). The protein (2 mg/ml) was cleaved at the Asp residues by incubation in 15 mM HCl for 2 h at 108 °C (23). For subsequent enzymatic digestion, the peptide mixture was brought to pH 7 with a sodium phosphate buffer (final concentration 25 mM) and digested overnight with sequencing grade endoproteinase Glu-C (Roche Applied Science) at a protease:substrate ratio of 1:30 (w/w). For reduction and alkylation, the peptides were treated with 5 mM dithiothreitol in 25 mM sodium phosphate buffer, pH 8, for 1 h at 56 °C followed by addition of 20 mM iodoacetamide (final concentration) and incubated at room temperature in the dark for 1 h. Peptide samples were either diluted to an equivalent of 0.2–2 pmol of protein/µl in 0.1% trifluoroacetic acid prior to LC/MS or LC/MS/MS or directly subjected to reversed-phase HPLC on a C$_{12}$ column. sGas1-ΔSer was cleaved at Asp in the same way as sGas2p. After cleavage the pH was raised to 6.5 with 50 mM PIPES buffer, and free cysteines were modified with 10 mM *N*-ethylmaleimide. Gas1p peptides were collected on Zip-Tips µC18 pipette tips (Millipore, Billerica, MA), washed with 0.1% trifluoroacetic acid, and eluted with a solution containing 50% v/v acetonitrile and 0.1% v/v trifluoroacetic acid.

Reversed-phase HPLC—A Jupiter Proteo C$_{12}$ column (inner diameter 2 mm, length 150 mm, Phenomenex, Torrance, CA) was operated on a SMART system with a fraction collector (Amersham Biosciences). A constant flow rate of 50 µl/min was maintained. After injection of the sample, the column was rinsed with 0.1% trifluoroacetic acid in water (solvent A) for 9 min. Peptides were eluted by applying a linear gradient to 50% acetonitrile in 0.1% trifluoroacetic acid (solvent B) over 75 min. Absorbance of the effluent was continuously recorded at 214, 254, and 280 nm. Fractions of 50 µl were collected, beginning 24 min after the start of the gradient.

Partial Reduction, Cyanylation, and Cleavage—Peptides in HPLC fractions were partially reduced in a medium containing 1 mM tris(2-carboxyethyl)phosphine (TCEP) (BioVectra, Oxford, CT) and 0.1 M sodium acetate buffer, pH 3, for 15 min

---

[3] The abbreviations used are: GPI, glycosylphosphatidylinositol; AGE, affinity gel electrophoresis; BSA, bovine serum albumin; CDAP, 1-cyano-4-dimethylaminopyridinium tetrafluoroborate; ER, endoplasmic reticulum; ERAD, ER-associated protein degradation; HPAEC, high performance anion-exchange chromatography; LC, liquid chromatography; ESI, electrospray ionization; FTICR, Fourier transform ion cyclotron resonance; MS, mass spectrometry; MS/MS, tandem mass spectrometry; PNGaseF, peptide *N*-glycosidase F; QTOF, quadrupole time-of-flight; TCEP, tris(2-carboxyethyl)phosphine; PIPES, 1,4-piperazinediethanesulfonic acid; HPLC, high pressure liquid chromatography; NtD, N-terminal domain.

at room temperature (24, 25). Then 10 mM 1-cyano-4-dimethylaminopyridinium tetrafluoroborate (CDAP) (Sigma) in 0.1 M acetic acid was added to cyanylate cysteine residues. The reaction mixture was incubated for 30 min at room temperature. Addition of CDAP also instantaneously inactivates TCEP under these conditions (26). Cleavage of cyanylated peptides was accomplished by adding 1 M ammonia and incubation at room temperature for 1 h (24). Reaction was stopped by the addition of 4.5 parts of 2.4% (v/v) trifluoroacetic acid before analysis by LC/MS on a QTOF mass spectrometer.

Mass Spectrometry—Mass spectra were analyzed with Virtualmslab to identify candidate disulfide-linked and linear peptides from sGas1-ΔSer and sGas2p. virtualmslab can perform multistage virtual experiments, in any user-defined order, with mass spectrometric analyses. The virtual experimental results are used to generate MS reference data bases that can be matched with the real MS data obtained from the equivalent real experiment (22). The settings for a quest for disulfide-linked peptides containing one disulfide bond or for linear peptides in sGas2p were as follows: cleavage at N-terminal and C-terminal peptide bonds at Asp with up to four missed cleavages allowed, cleavage at the C-terminal peptide bond at Glu, except at Glu-Pro, with up to one missed cleavage allowed; free cysteines modified by iodoacetamide. For sGas1-ΔSer the settings were as follows: cleavage at Asp, optional conversion of Asn to Asp (as a result of deglycosylation by PNGaseF), and cleavage at newly formed Asp, up to four missed cleavages at Asp allowed; free cysteines modified by N-ethylmaleimide.

Peptides were separated on a reversed-phase C18 PepMap analytical column (inner diameter 75 μm, length 150 mm) operated on an Ultimate nano-LC system (LC Packings Dionex, Sunnyvale, CA) at a flow rate of 300 nl/min using a gradient of 1–50% acetonitrile, 0.1% formic acid. The eluate was directly electrosprayed in a quadrupole time-of-flight mass spectrometer (Waters) operating in MS-alone mode or in data-dependent MS/MS mode. Fragmentation was conducted with argon as collision gas at a pressure of 4×10^{-5} bars. Tandem mass spectrometric spectra were processed with the MaxEnt3 algorithm embedded in Masslynx Proteinlynx (Waters) software to generate peak lists used to search the *S. cerevisiae* mass spectrometry protein sequence data base (MSDB, Imperial College, London, UK) using the Mascot search engine (Matrix Science, London, UK). Peptide mass tolerance and fragment mass tolerance were set at 0.2 Da, and cleavage at each peptide bond was allowed. Gas2p peptides cleaved at Asp or Glu thus identified were used as internal calibrants for mass spectra acquired with FTICR mass spectrometry (see below). Analysis of MS/MS spectra of candidate disulfide-linked precursor ions was supported by the Biolynx tool of the Masslynx software by editing one cysteine-containing candidate peptide as a modification on the cysteine residue of the other candidate and vice versa. Theoretical possible fragments were predicted and compared with the raw data.

LC/electrospray ionization/FTICR-MS data were acquired with an ApexQ Fourier transforms ion cyclotron mass spectrometer (Bruker Daltonics, Bremen, Germany) equipped with a 7T magnet and a CombiSource[TM]. The mass spectrometer was coupled to a 200-μm inner diameter, 750-mm long mono-

lithic reverse phase column (GL Sciences, Tokyo, Japan) operated on an Ultimate 2000 HPLC system at a flow rate of 2 μl/min. Following injection of the sample (1 μl), a linear solvent gradient was applied in 30 min from 100% H_2O, 0.1% formic acid to 50% H_2O, 50% acetonitrile, 0.1% formic acid, during which about 600 high resolution mass spectra were recorded. Mass calibration was accomplished using LC-QTOF-MS/MS validated peptides as internal calibrants, resulting in a mass accuracy of better then 2 ppm over the complete MS data set. Mass spectra were charge-deconvoluted, and the resulting data set composed of 308 peptide ion chromatograms with corresponding masses and retention times was imported in the virtualmslab program.

Tandem mass spectrometry data on the FTICR mass spectrometer were acquired with off-line nano-electrospray using a 2-μl sample in a nano-electrospray needle with a 2-μm (inner diameter) tip (New Objectives, Woburn, MA). Multiple charged peptides were mass selected in the quadrupole sector and then accelerated with 12 V into the hexapole collision cell for collisional dissociation at an argon pressure of about 5×10^{-6} mbars (pressure gauge reading). The resulting fragment ions were accumulated for 2 s and then extracted from the collision cell and injected into the ICR cell for mass analysis. Matrix-assisted laser ionization/desorption-FTICR mass analysis was performed as described previously (22).

Expression and Purification of Recombinant Gas Proteins—pHIL-S1-derived plasmids, linearized with BglII, were transformed into *Pichia pastoris* strain GS115 (*his4*), and the selection of His[+]Mut[s] mutants and protein induction were performed as described previously (27). Large scale purification of His[6]-tagged Gas1 proteins by nickel-nitrilotriacetic acid affinity chromatography was performed under native conditions. About 400 ml of the culture supernatant was concentrated to 1/10th of the original volume by ultrafiltration through a Millipore regenerated cellulose membrane (cutoff 30,000). The concentrated fraction was dialyzed against Lysis Buffer (LB) (50 mM sodium phosphate buffer, pH 8.0, 200 mM NaCl) at 4 °C overnight. Two ml of 50% nickel-nitrilotriacetic acid (1 ml of resin (Qiagen) plus 1 ml of LB) was added to the dialyzed fraction and left at 4 °C for 1 h (27) under gentle agitation. A mixture of protease inhibitors (Roche Applied Science) was added at each step. Then the mixture was loaded onto a column (1 × 10 cm, Econo Bio-Rad column) and washed twice with 16 ml of Wash Buffer (50 mM sodium phosphate buffer, pH 8.0, 200 mM NaCl, 3–5 mM imidazole). To elute the protein, the column was washed four times with 1 ml of Elution Buffer (50 mM sodium phosphate buffer, pH 8.0, 200 mM NaCl, 200 mM imidazole). The column flow-through, wash, and elution fractions were collected, and protein content was determined by the dye reagent protein assay (Bio-Rad).

Deletion Analysis—Recombinant plasmids for integrative recombination in *P. pastoris* were generated by cloning BamHI/XhoI-digested PCR fragments into the corresponding sites of the expression vector, pHIL-S1, to obtain in-frame fusion with the secretion signal of the *P. pastoris PHO1* gene. The plasmid pXH, carrying the full coding sequence of the *GAS1* gene, was used as template for PCR amplifications (28). The His[6]-tagged soluble forms, Gas1-Δ8Cys and Gas1-ΔL, were obtained using

the forward primer XHup (5′-GCATATTCGACTGA<u>CTC-GAG</u>AACGATGTTCCAGCGATTGAA-3′) and the reverse primers Δ8Cys-rev (5′-ATCGTCCTCA<u>GGATCC</u>**TTA***GT-GATGGTGATGGTGATG*GCCTCCGTTTGGAGT-3′) or ΔL-rev (5′-ATCGTCCTCA<u>GGATCC</u>**TTA***GTGATGGTGAT-GGTGATG*TGTGTTGGCGGAAGTTGG-3′), respectively. XHup is complementary to nucleotides +68 to +87 of the coding region of *GAS1* and has an XhoI site incorporated (underlined). Δ8Cys-rev and ΔL-rev are complementary to nucleotides +1090 to +1104 and to nucleotides +990 to + 1008, respectively. These primers have an in-frame His$_6$ coding sequence (shown in italics), a TAA stop codon (shown in boldface), and a BamHI site (underlined). The plasmid G2, carrying the full coding sequence of the *GAS2* (17), was used as template for PCR amplifications. The His$_6$-tagged soluble form, Gas2-Δ8Cys, was obtained using the forward primer Gas2-XhoI (5′-AGCATATTCGACTGA<u>CTCGAG</u>GTGTCAGCTTTGA-AAAAACC-3′) and the reverse primer Gas2-ΔCys-rev (5′-ATCGTCCTC<u>GGATCC</u>**TTA***GTGATGGTGATGGTGAT-GG*CTTCTATCAGGTGTTT-3′). Primer Gas2-XhoI is complementary to nucleotides +78 to +99 of the coding region of *GAS2* and has an XhoI site incorporated (underlined). Gas2-Δ8Cys-rev is complementary to nucleotides +1148 to +1164 and has an in-frame His$_6$ coding sequence (shown in italics), a TAA stop codon (shown in boldface), and a BamHI site (underlined).

Different recombinant plasmids for the expression and secretion of His$_6$-tagged forms of the 8Cys-box of Gas1p in *P. pastoris* were derived from the pHILS-1 or PICZαA vectors (Invitrogen). Three constructs were obtained as follows: (i) from Asn^{366} to Gly^{486}; (ii) from Ala^{357} to Gly^{486}; and (iii) from Ala^{350} to Asp^{482}. Oligonucleotide sequences used for PCR amplifications are available upon request.

Plasmid DNA was purified using commercial purification kits (Qiagen). DNA sequencing was used to confirm the correct fusions and the absence of undesired mutations throughout the coding sequence (BMR Genomics, Università di Padova, Padova, Italy). Standard procedures using lithium acetate were used for yeast transformation.

Mutagenesis of Cys^{348}—The mutant GPI-anchored form Gas1-C348S was constructed by a PCR-based cassette mutagenesis. A fragment of *GAS1* gene was amplified using the primer pair Gas1Prom (5′-<u>TCGAGCTC</u>GAAGGAATCTTC-CAACCT-3′), complementary to nucleotides −597 to −580 from the start codon, and C348SG1R (5′-TACTTA<u>CCAG-TAGCTGG</u>**ACT**AGCAACATCACTTGTTGTT-3′), complementary to nucleotides +1041 to +1003. Gas1Prom has a SacI site (underlined), whereas C348SG1R has a *Van91*I site (underlined) and a serine codon (in boldface) instead of the Cys^{348} codon (TGT). Expand High Fidelity PCR system (Roche Applied Science) was used for the amplification from yeast genomic DNA. The mutant fragment of the *GAS1* gene was cloned into the PCRII-TOPO-*GAS1* plasmid harboring the wild-type *GAS1* (−597/+2024) and previously digested with SacI/Van91I to remove the 5′ part of the *GAS1* gene. The resulting plasmid (PCRII-TOPO-*GAS1*C348S) was SacI/BamHI-digested to excise the *GAS1*-C348S mutant gene and clone it into the SacI/BamHI-digested YCplac33 yeast single

copy vector. The plasmid was used to transform the WB2d (*gas1::LEU2*) strain of *S. cerevisiae*. As a control, the same strain was transformed with the wild-type *GAS1* gene cloned in the same vector (−597/+2024 fragment).

Enzyme Assays—β(1,3)-Endoglucanase activity was measured by the reducing sugar assay using the *p*-hydroxybenzoic acid hydrazide reagent with borohydride-reduced laminarin (5). The purified protein fractions were dialyzed against 50 mM sodium acetate buffer, pH 5.5, at 4 °C, and 10 μg of purified protein was incubated with 40 μl of reduced laminarin (10 mg/ml) in 50 mM sodium acetate buffer, pH 5.5, in a final volume of 0.5 ml. At different times, 50 μl of the reaction mixtures were withdrawn and kept at 4 °C. Then 950 μl of *p*-hydroxybenzoic acid hydrazide solution was added to the samples and to the glucose standards. After 10 min of boiling the absorbance at 405 nm was measured. To test for β(1,3)-glucanosyltransferase activity, 1–1.5 μg of the purified protein were incubated with 3 mM reduced laminarioligosaccharide containing 13 glucose residues (rG$_{13}$), and the assay was performed as described previously (27). Aliquots of 2.5 μl were withdrawn at different times (0-1-2-4-8 and 24 h), supplemented with 47.5 μl of 50 mM NaOH and then analyzed by HPAEC through a CarboPAC-PA1 column (Dionex 4.6 × 250 mm) as described by Hartland *et al.* (5). The activity was determined by measuring the difference in the surface area of the substrate peak (rG13) in a HPAEC profile, normalized for the total surface area of the peaks, between two different time points at the beginning of the reaction. In this time the contribution of the transferase products, which are themselves substrates, to the activity is negligible. β(1,3)-Glucanosyltransferase activity was expressed as μmol of rG13 consumed h^{-1}/mg of purified protein.

Electrophoresis and Immunoblotting Procedures—Aliquots of *P. pastoris* culture supernatants or fractions from the purification procedure were denatured by boiling for 3 min in SDS sample buffer (0.0625 M Tris-HCl, pH 6.8, 2.3% (w/v) SDS, 5% (v/v) 2-mercaptoethanol, 10% (v/v) glycerol). Total protein extracts from *S. cerevisiae* cells were obtained as described previously (29). The medium fraction (50 ml) was collected when exponentially growing cells reached an $A_{450\,nm}$ of about 1. Proteins secreted into the medium were obtained by cold trichloroacetic acid precipitation using BSA as a carrier (2 μg/ml) as described previously (30).

Proteins were separated by SDS-PAGE on 8% polyacrylamide gel. After electrophoresis, gels were stained with Coomassie Blue R-250 or with silver nitrate (silver staining kit, Amersham Biosciences). Immunoblotting was performed as described previously (31) using anti-polyhistidine tag monoclonal antibody (1:1,500) (Novagen, Madison, WI), anti-Gas1p rabbit serum at a 1:2,000 dilution, and anti-actin monoclonal antibody clone at 1:1,000 (MP Biomedicals, Aurora, OH). Peroxidase-conjugated anti-rabbit (1:10,000) or anti-mouse (1:5,000) affinity-purified F(ab′)$_2$ fragments of donkey IgGs were from Jackson ImmunoResearch. Bound antibodies were revealed with the ECL Western blotting detection reagents (Amersham Biosciences).

Affinity Gel Electrophoresis and Assay of Binding to the Cell Wall—Affinity gel electrophoresis (32) was carried out in 12% polyacrylamide gel polymerized in the absence or presence of
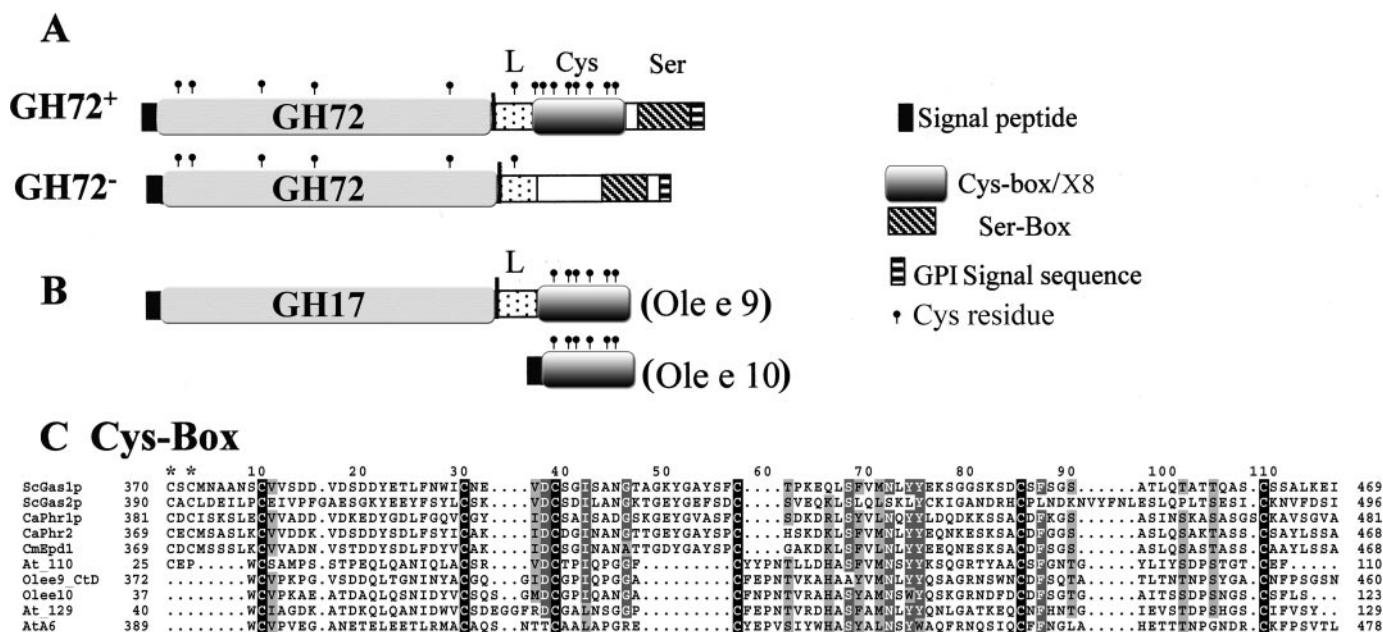
FIGURE 1. **Scheme of the modular organization of GH72 proteins.** The amino acid sequences of 90 proteins of family GH72 were analyzed. *A*, representative scheme of the GH72 subfamilies. ● indicates the position of a conserved Cys residue. *B*, organization of domains of plant proteins containing a Cys-box/X8 domain. As examples Ole e 9 and Ole e 10 polypeptides from olive tree (*Olea europaea*) pollen are shown. *C*, representative alignment of the Cys-box of yeast and plant proteins. *Sc, Saccharomyces cerevisiae; Ca, Candida albicans; Cm, Candida maltosa; At, Arabidopsis thaliana.* The multiple alignment was obtained by ClustalW and manually edited to align the cysteine residues. The *asterisk* denotes the cysteine residues conserved in the GH72+ proteins.

various amounts (0–0.5% w/v) of laminarin from *Laminaria digitata* (Sigma). BSA was used as a control. Purified proteins (1.5–5 μg) were added with glycerol and bromphenol blue prior to loading. The gel was prepared in Tris-HCl buffer (0.4 M Tris-HCl, pH 8.8), and gels were run in parallel in running buffer (0.025 M Tris-HCl, 0.192 M glycine, pH 8.3). Electrophoresis was performed at 100–150 V for 1.5 h at 4 °C. After the run, gels were stained with Coomassie Blue. Binding to laminarin was assessed visually. For the binding assays to the yeast cell wall β(1,3)-glucan, 2 μg of purified sGas1p or sGas1-ΔSer were incubated for 30 min at 4 °C in 5 mM acetate buffer, pH 5.5, with 10 or 50 mg (wet weight) of alkali-insoluble fraction of cell walls obtained, as described previously (33), and washed once with 100 mM Tris-HCl, pH 7.5, twice with 10 mM Tris-HCl, pH 7.5, and twice with 5 mM sodium acetate, pH 5.5. Aliquots of the input and of the supernatant and pellet obtained after a centrifugation at 15,000 × g for 5 min were analyzed by immunoblot using anti-Gas1p antibodies. As controls, samples with cell walls alone, protein alone, and BSA were set up.

Pulse-Chase Experiment and Immunoprecipitation—Logarithmically growing cells, corresponding to 12 $A_{450 nm}$, were pulse-labeled as described previously (27) with the exception that 400 μCi of Express-[35S] Protein Labeling Mix (PerkinElmer Life Sciences) were used instead of [35S]methionine. The chase solution contained 0.3% (w/v) methionine, 0.3% (w/v) cysteine, and 0.3 M (NH$_4$)$_2$SO$_4$. At the end of the pulse the amount of radioactivity incorporated by the cold trichloroacetic acid-precipitable material was determined. Immunoprecipitation of Gas1p was performed as described previously (27).

Circular Dichroism—CD spectra were obtained as described previously (27). Secondary structure estimations were performed by computer fit according to the method of Perczel *et al.* (34). Thermal unfolding of truncated proteins was moni-

tored by recording the ellipticity at 220 nm while heating from 20 to 80 °C at 1 °C/min with a computer-controlled circulation water bath.

Secondary Structure Prediction—The domain boundaries of the Gas2 Cys-box were predicted by alignment of multiprotein families extracted from X8 domain of Pfam protein families data base (35, 36). Nine residues starting at Cys[390] were added at the N terminus of the X8 domain of Gas2p. Secondary structure was predicted using the structure prediction methods PSIPRED (37) and Jnet (38).

RESULTS

Sequence Features of GH72 Proteins and Cys-box/X8 Domain—Members of the GH72 family share a cleavable signal peptide and a GH72 signature domain annotated in the CAZy and Pfam Databases (Fig. 1*A*). Here we refer to this domain as the NtD. It contains the following: (i) two conserved glutamate residues that are essential for the catalysis (6, 27, 39); (ii) a conserved pattern of five Cys residues; and (iii) a predicted TIM $(\alpha/\beta)_8$ barrel fold (40). This domain is followed by a putative linker in which a Cys residue is strikingly conserved in an otherwise poorly conserved context (marked "*L*" in Fig. 1*A*). Subfamily 72+ shares a Cys-box that is annotated in Pfam as the X8 domain family, whereas GH72− lacks this domain (Fig. 1*A*). The Cys-box/X8 domain is unique to fungal and plant extracellular proteins. Closer inspection suggests that the amino acid similarity of the Cys-box/X8 domain from GH72+ proteins and from plant proteins is rather weak. As an example, the Cys-box of Gas1p and Gas2p shares an amino acid identity of 23–25% with the X8 domain of the well characterized Ole e 10 or Ole e 9 proteins of olive pollen, a lectin and a β(1,3)-glucanase of GH17 family, respectively (see Fig. 1*B*) (41, 42). Remarkably, the fungal Cys-box has a short N-terminal extension where two

TABLE 1

LC-ESI-FTICR mass spectrometry of Gas2p peptides with a single disulfide bond, obtained by chemical cleavage at Asp and enzymatic cleavage at Glu

Disulfide bond	Observed mass (M + H$^+$)	Relative intensity	Theoretical mass (M + H$^+$)	Peptide sequences	Amino acid numbering
		%			
Cys^{89}–Cys^{118}	1221.6144	1.1	1221.6152	<u>PKICLR</u>, <u>ICME</u>^{a}	86–91, 117–120
	1336.6396	4.6	1336.6422	PKICLRD, ICME^a	86–92, 117–120
	2001.9523	14.1	2001.9555	PKICLR, DPTKSHDICME^a	86–91, 110–120
Cys^{231}–Cys^{367}	2465.1754	6.7	2465.1741	<u>NLARYFVCG</u>, <u>SVECPHIAVGVWE</u>^{a}	224–232, 363–376
	2580.1997	11.7	2580.2010	DNLARYFVCG, SVECPHIAVGVWE^a	223–232, 363–376
	2878.4009	1.3	2878.4015	NLARYFVCGDVKA, SVECPHIAVGVWE	224–236, 363–376
	2993.4249	2.9	2993.4284	DNLARYFVCGDVKA, SVECPHIAVGVWE	223–236, 363–376
				or	
				NLARYFVCGDVKAD, SVECPHIAVGVWE	224–237, 363–376
	3039.4260	3.9	3039.4274	AMTRDNLARYFVCG, SVECPHIAVGVWE^a	219–232, 363–376
	3154.4507	15.3	3154.4543	AMTRDNLARYFVCGD, SVECPHIAVGVWE^a	219–233, 363–376
	3269.4756	2.0	3269.4813	DAMTRDNLARYFVCGD, SVECPHIAVGVWE	218–233, 363–376
Cys^{247}–Cys^{278}	3162.4211	1.4	3162.4197	<u>WCGYSTYGTSGYRE</u>, <u>FGCNLVRPRPFTE</u>^{a}	246–259, 276–288
Cys^{399}–Cys^{466}	2139.0345	2.6	2139.0362	ILPCEIVPFGAE, DRHCPLN	396–407, 463–469
				or	
				ILPCEIVPFGAE, RHCPLND	396–407, 463–469
	2433.1651	1.4	2433.1690	ILPCE, RHCPLNDKNVYFNLE	396–400, 464–478
	3146.5397	20.4	3146.5438	<u>ILPCEIVPFGAE</u>, <u>RHCPLNDKNVYFNLE</u>^{a}	396–407, 464–478
Cys^{419}–Cys^{424}	1412.5850	6.5	1412.5861	<u>YFSYLCSKVDCS</u>^{a}	414–425
	1430.5942	1.2	1430.5967	YFSYLCSKVD, CS^a	414–423, 424–425
	1527.6101	12.8	1527.6131	YFSYLCSKVDCSD^a	414–426
	1545.6214	3.7	1545.6236	YFSYLCSKV, DCSD	414–422, 423–426
				or	
				YFSYLCSKVD, CSD	414–423, 424–426
	2314.0720	7.8	2314.0730	YFSYLCSKV, CSDILANGKTGE	414–422, 424–435
	2411.0881	71.6	2411.0894	YFSYLCSKVDCSDILANGKTGE^a	414–435
	2429.0991	20.7	2429.1000	YFSYLCSKV, DCSDILANGKTGE^a	414–422, 423–435
	2540.1272	2.3	2540.1320	EYFSYLCSKVDCSDILANGKTGE	413–435
	2760.2149	1.7	2760.2168	YFSYLCSKVDCSDILANGKTGEYGE	414–438

^{a} Structure was confirmed by MS/MS. MS/MS fragment spectra of underlined disulfide-linked peptides are shown in supplemental Fig. S2).

close Cys residues, which do not align with the plant X8, are present (indicated by an *asterisk* in Fig. 1*C*). This suggests that the domain size of fungal X8 could be larger and involve a pattern of eight cysteine residues (8Cys) instead of the six (6Cys) typical of the plant X8 domain. In total, GH72$^+$ enzymes share a pattern of 14 regularly spaced Cys residues, six of which fall in the NtD + L region and eight in the Cys-box. Previous work showed the existence of intramolecular disulfide bridges in Gas1p (27).

In this work we have focused on the characterization of disulfide bonds in Gas1 and Gas2, two homologous GH72$^+$ proteins of *S. cerevisiae* that share 53% of amino acid identity in the NtD+L region, and 41% in the remaining part of the protein. Both proteins exhibit identical *in vitro* activity (17).

Mapping Disulfide Bonds in Gas2p—Our initial attempts at determining the position of the disulfide bridges in Gas1p were unsatisfactory. Analysis of a matrix-assisted laser ionization/ desorption-FTICR mass spectrum of peptides obtained by chemical cleavage at pH 2 of purified sGas1-ΔSer (see the construct in Fig. 5*A*), treated with PNGaseF to remove the *N*-linked glycan chains, revealed the presence of candidate peptides containing Cys^{74}–Cys^{104} and Cys^{398}–Cys^{403} disulfide bonds. However, further analysis was hampered because of the presence of many *O*-linked glycans and the lack of suitable cleavage sites between residues Cys^{370}, Cys^{372}, and Cys^{379}. Therefore, we turned our attention to Gas2p that is less mannosylated and contains more suitable cleavage sites. We used a soluble form of Gas2p (sGas2p), containing a His$_6$ tag at the C terminus in place of the GPI-anchor signal (Fig. 5*B*) (17). Free –SH groups were first alkylated with iodoacetamide, and the alkylated protein was dialyzed against water, cleaved at pH 2 at 108 °C, and then

digested with endoproteinase Glu-C at pH 7. The digest was subjected to LC/FTICR-MS for accurate mass measurement. Mass spectra were analyzed with the software program Virtualmslab to identify candidate disulfide-linked peptides. Virtualmslab suggested 23 structures with an intra- or inter-peptide disulfide linkage, distributed over five possible disulfide bridges with a mass accuracy of 2 ppm or better (Table 1). The peptide mixture was also subjected to LC/MS/MS. Fourteen candidate peptides with a disulfide bond were selected for collision-induced dissociation. By manual inspection of the fragment ion spectra, the identities of all 14 were confirmed (Table 1 and supplemental Fig. S2). The consistency of these results indicates that the five linkages listed in Table 1 are native disulfide bonds in the protein and that scrambling had not occurred.

Until this point, we had observed neither peptides with a free Cys residue nor Cys residues modified with iodoacetamide, even considering a peptide containing Cys^{457}, the only Cys residue in Gas2p that is not conserved in the family of GH72$^+$ enzymes and is therefore expected to be alkylated as it is unlikely to be involved in a disulfide bond. It is possible that a signal from such a peptide was present in the mass spectrum but that the corresponding compound bore an unknown modification and therefore was not nominated by Virtualmslab. On the other hand, after reduction with dithiothreitol and alkylation with iodoacetamide, most peptides from native disulfide-bonded species were detected by LC/MS and LC/MS/MS with the Cys residue properly modified. In addition, we identified two cleavage variants of a peptide alkylated at Cys^{442} (FSDCSVE and YGEFSDCSVE), two cleavage variants of a peptide alkylated at Cys^{489} (SICKNFV and SICKNFVD), and three cleavage variants of a peptide alkylated at Cys^{390} and Cys^{392}

(RSKCACLDE, KLPETPDRSKCACLDE, and ANEKLPETP-DRSKCACLDE). This indicated that these peptides are also involved in disulfide linkage, bringing the total number of disulfide bonds in Gas2p to seven. No evidence for the presence of peptides with a Cys^{442}–Cys^{489} disulfide bond or for an intrapeptide S–S bond between Cys^{390} and Cys^{392} was found in the peptide mixture before reduction and alkylation. On the contrary, the LC/FTICR-MS mass spectrum of the peptide mixture before reduction and alkylation contained several peaks with *m/z* values compatible with peptide ions containing two disulfide bonds in which Cys^{390}, Cys^{392}, Cys^{442}, and Cys^{489} are involved. To confirm the identity of these species, the peptide mixture was fractionated by HPLC, and a fraction enriched in disulfide-bonded peptides containing Cys^{390}, Cys^{392}, Cys^{442}, and Cys^{489} was subjected to off-line MS/MS on the FTICR-MS mass spectrometer. One of the candidates, a peptide of *m/z* 4183.84 ($(M + H)^+$) was selected for collision-induced dissociation. The MS/MS spectrum of the parent ion in the 5^+ charge state (Fig. 2) allowed assessment of the expected identity but showed no evidence for the presence of fragment ions resulting from cleavage of a peptide bond between Cys^{390} and Cys^{392}, preventing identification of the disulfide linkages in this peptide. To map the disulfide bonds between Cys pairs involving Cys^{390}, Cys^{392}, Cys^{442}, and Cys^{489}, we applied a method using partial reduction of disulfide bonds by TCEP, at low pH to prevent –SH-catalyzed disulfide rearrangement, followed by cya-

nylation of Cys residues by CDAP and ammonia-induced cleavage at cyanylated Cys residues (24). The cleavage reaction yields an N-terminal peptide with an amide group at its C terminus and a C-terminal peptide with an iminothiazolidine modification at the N terminus. An HPLC fraction containing six variants of the peptide with disulfide bonds at Cys^{390} and Cys^{392} was subjected to this treatment and analyzed with LC/MS. Results revealed that Cys^{390} is connected to Cys^{442} and Cys^{392} to Cys^{489}. All six expected N-terminal ammonia-induced cleavage products and both expected C-terminal cleavage products of the six variants were detected with high mass accuracy, whereas none of the products pointing to the opposite disulfide bond arrangement could be observed at *m/z* values within the mass accuracy of the instrument (Table 2).

The arrangement of all seven intramolecular disulfide bonds in Gas2 protein is summarized in Fig. 3 (*top*). One network of three disulfide bridges connects the six Cys residues inside the NtD + L region, five belonging to NtD and one (Cys^{367}) to L, and another one of four connects the eight cysteine residues of the Cys-box. This strongly supports the existence of a module with an eight Cysteine pattern (8Cys-box) in the yeast proteins. The disulfide bonds of Gas1p deduced from the arrangement of disulfide bridges of Gas2p are shown in Fig. 3 (*middle*). The Cys of the L region in Gas1p is Cys^{348}.

Recently a model of the structure of the NtD of Gas1p was reported (40). The model is compatible with the Cys^{89}–Cys^{118} and the Cys^{247}–Cys^{278} disulfide bonds in this domain of Gas2p. Interestingly, the conserved Cys^{367} residue in the L region is connected to Cys^{231} in the NtD and could not be taken into account by the model. This configuration suggests that the 8Cys-box may be closely associated with the NtD rather than forming an independent appendix.

The solution NMR structure of the C-terminal domain of the pollen antigen Ole e 9, comprising the X8 domain, was recently presented (43). Comparison of the disulfide structure of the C-terminal domain of Ole e 9 with the results described here show that two disulfide bonds are conserved between the Pfam X8 domain of Ole e 9 and the Cys-box of Gas2p. These include the Cys^{373}–Cys^{435} (Ole e 9) and the corresponding Cys^{399}–Cys^{466} (Gas2p) disulfide bond, and the Cys^{392}–Cys^{398} (Ole e 9) and the corresponding Cys^{419}–Cys^{424} (Gas2p) bridge. In Ole e 9 the remaining two conserved Cys residues are directly linked to each other, forming
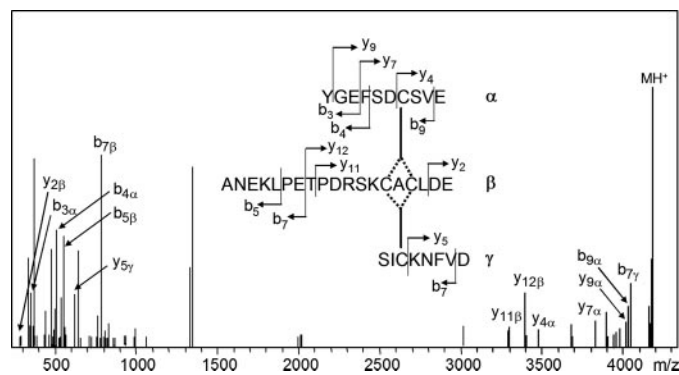

FIGURE 2. **Fragment ions obtained by collision-induced dissociation of an *m/z* 4173.842 (M + H$^+$) precursor ion confirm the proposed peptide composition and presence of two disulfide bonds but do not allow identification of the linked cysteine pairs.** Identification was accomplished by partial reduction, cyanylation, ammonia-induced cleavage, and mass analysis of this peptide and a number of cleavage variants of this peptide (see Table 2).

TABLE 2

LC-ESI-QTOF mass spectrometry of ammonia-induced cleavage products from cyanylated partially reduced Gas2p peptides with two disulfide bonds comprising Cys^{390}, Cys^{392}, Cys^{442}, and Cys^{489}

The abbreviation itz means iminothiazolidine derivative. Listed cleavage products show that Cys^{390} is connected to Cys^{442} and Cys^{392} to Cys^{489}. No products derived from peptides with a Cys^{390}–Cys^{489} or a Cys^{392}–Cys^{442} disulfide bond were detected within 10 ppm from theoretical masses, *i.e.* the mass accuracy of the QTOF mass spectrometer under these conditions.

| Disulfide bond	Observed mass (M + H$^+$)	Theoretical mass (M + H$^+$)	Mass deviation	Peptide sequences	Amino acid numbering
			ppm		
Cys^{390}–Cys^{442}	1346.580	1346.583	−2	RSKCA-amide, FSDCSVE	387–391, 439–445
	1695.712	1695.710	1	RSKCA-amide, YGEFSDCSVE	387–391, 436–445
	2126.966	2126.984	−9	KLPETPDRSKCA-amide, FSDCSVE	380–391, 439–445
	2476.093	2476.112	−7	KLPETPDRSKCA-amide, YGEFSDCSVE	380–391, 436–445
	2441.107	2441.107	0	ANEKLPETPDRSKCA-amide, FSDCSVE	377–391, 439–445
	2790.220	2790.234	−5	ANEKLPETPDRSKCA-amide, YGEFSDCSVE	377–391, 436–445
Cys^{392}–Cys^{489}	1485.629	1485.617	8	itz-CACLDE, SICKNFV	390–395, 487–493
	1600.641	1600.644	−2	itz-CACLDE, SICKNFVD	390–395, 487–494
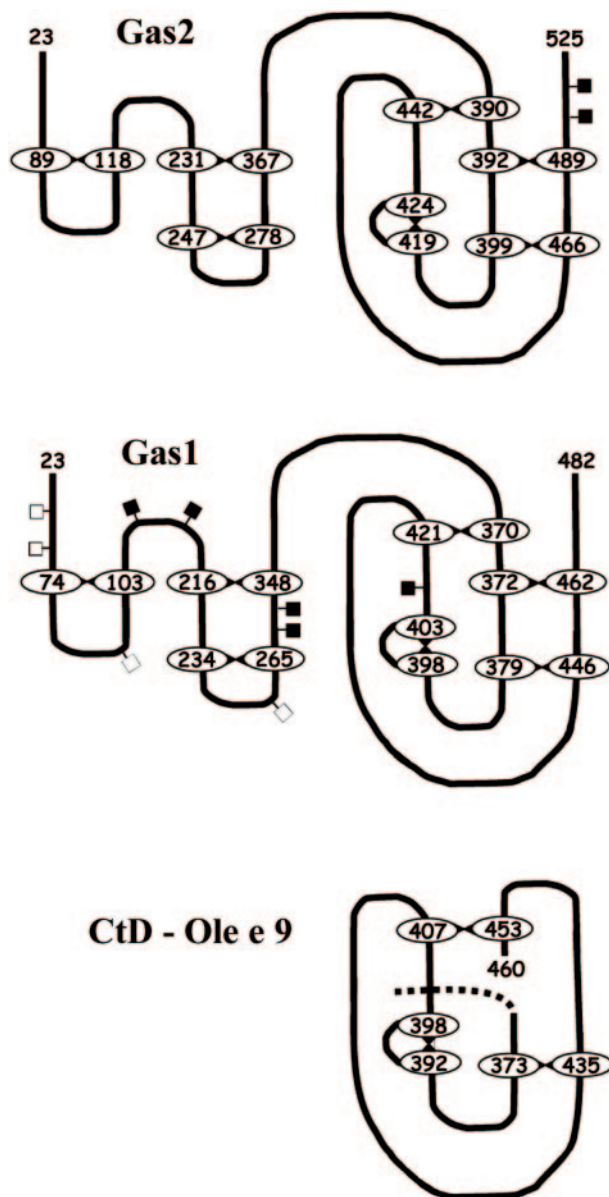
FIGURE 3. **Disulfide bond structure of Gas2p, Gas1p, and C-terminal domain of Ole e 9.** The Cys residues are shown as *numbered ovals*. ■ indicates a potential *N*-glycosylation site. □ marks the position of *N*-glycosylation as revealed by Asn to Asp conversion observed by mass analysis of peptides after PNGaseF treatment of sGas1-ΔSer.
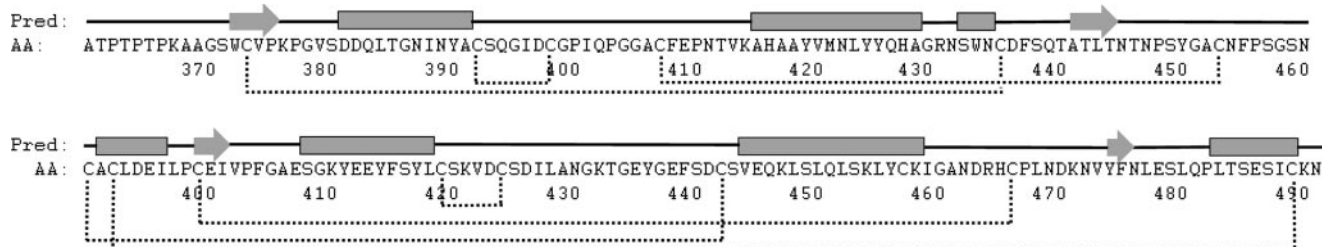
the Cys^{407}–Cys^{453} bond, while in Gas2p the corresponding Cys residues Cys^{442} and Cys^{489} are indirectly coupled, via the $^{390}CAC^{392}$ sequence in the N terminus of the Cys-box (Fig. 3). In Ole e 9, the N-terminal part seems to have a large degree of freedom. The connection of the N terminus of the Cys-box via Cys^{390} and Cys^{392} with the C-terminal half of the Cys-box by linkage to Cys^{442} and Cys^{489}, respectively, indicates a more defined spatial arrangement of these parts in the $GH72^{+}$ subfamily of glucanosyltranferases than in plant X8. Secondary structure prediction by various methods (37, 38) revealed that the two α-helices and two β-strands of the X8 domain of Ole e 9 are present in Gas2p at corresponding positions (Fig. 4). This indicates that at least part of the Cys-box has a fold similar to the X8 domain. In addition it is predicted that Gas2p possesses two additional α helices in the Cys-box, one being at the N-terminal end (containing Cys^{390} and Cys^{392}) and the other in the C-terminal part of the Cys-box and containing Cys^{489}. If present in the native proteins, these two α-helices should be held in close proximity by the Cys^{392}–Cys^{489} linkage, although it should be noted that the additional α-helix at the N terminus in Gas2p shows a low confidence estimate for the prediction. In conclusion, both secondary structure predictions and the cysteine connections in plant X8 domains and fungal Cys-boxes suggest a clear resemblance but also an important difference in overall three-dimensional structure that may be related to possible different functions of these domains. Therefore yeast 8Cys-box may constitute a subgroup in the X8 domain family. These differences prompted us to study the importance of the 8Cys-box and of the L region, containing the conserved Cys residue, for the expression, conformation, and enzyme activity of $GH72^{+}$ proteins in *S. cerevisiae*.

Truncation Analysis—We expressed C-terminally truncated mutants of Gas1p, sGas1 (lacking the GPI signal), and sGas1-ΔSer (lacking the Ser-box) in *P. pastoris,* under the control of the inducible *AOX1* promoter (see Fig. 5*A*) (27). Two further truncations were constructed as follows: sGas1-Δ8Cys, (lacking the 8Cys-box and ending at residue 368) and sGas1-ΔL (in which the L region was deleted and the protein was shortened to residue 336 where the prediction of the TIM barrel fold also ends). The truncated proteins carried a His_6 tag fused at the C-terminal end (not shown in Fig. 5). All proteins were secreted at a similar level with a yield of about 30–35 mg/liter of medium at 48 h of induction. A Coomassie-stained gel of the purified proteins is shown in Fig. 5*C*. The apparent molecular mass of
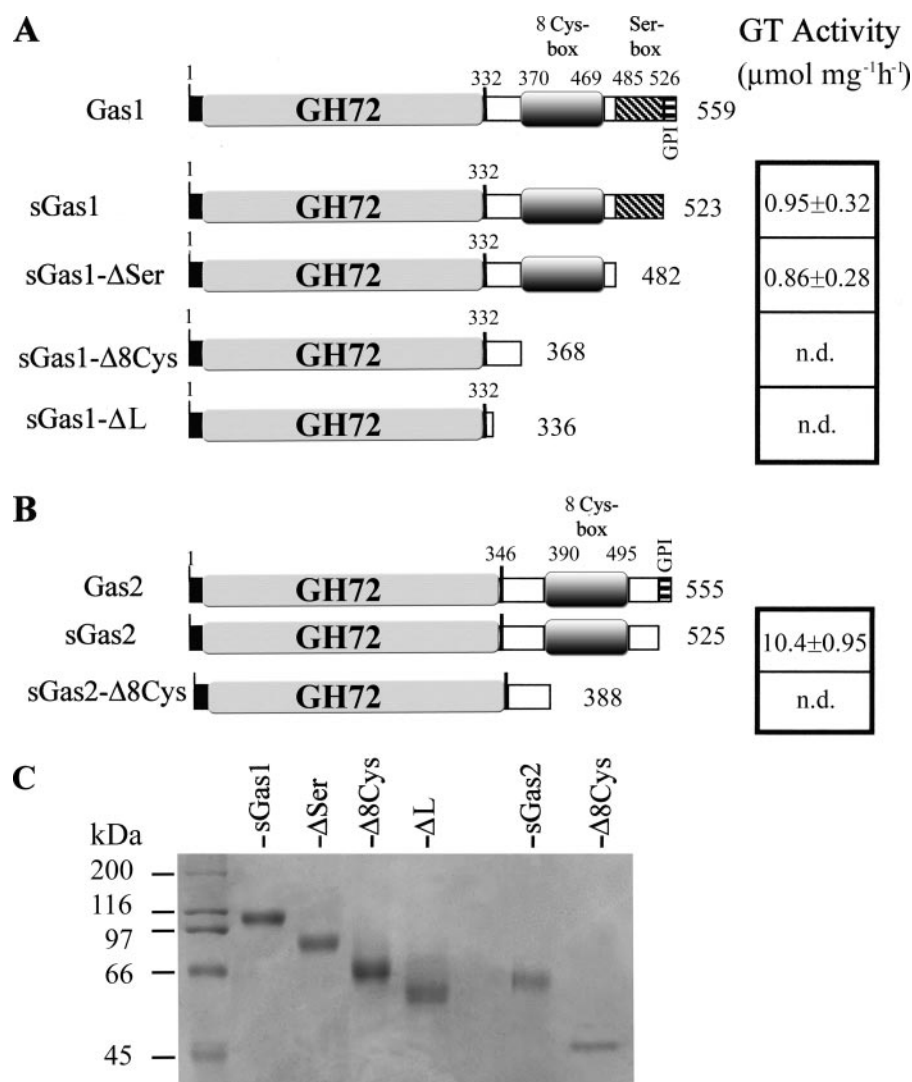

FIGURE 4. **Comparison of the secondary structure prediction of the 8Cys-Box of Gas2p (*lower panel*) with the secondary structure of the X8 domain of Ole e 9 (*upper panel*).** The *boxes* represent the α-helix and the *arrows* the β-strand. The *dotted lines* indicate a disulfide bond between two cysteine residues. Because the $^{390}CAC^{392}$ motif of Gas2p was not included in the Pfam domain boundary prediction of X8 domain (PF07983), nine residues were manually added at the N terminus of the Gas2p X8 domain, and they appear to constitute the first α-helix as predicted by Jnet and PSIPRED. The experimentally determined structure of the CtD of Ole e 9 is described in Ref. 43.

FIGURE 5. **Schematic diagram of the C-terminal constructs of Gas proteins.** *A*, different constructs of Gas1p were placed under the control of the *AOX1* methanol-inducible promoter and expressed in *P. pastoris* strain GS115 in a soluble (prefix s) and His$_6$-tagged form. The *black boxes* represent the N-terminal signal peptide, and the *horizontal stripe boxes* represent the C-terminal GPI attachment signal. *B*, scheme of the Gas2p truncated forms. *C*, Coomassie Blue-stained SDS-slab gel of 5 μg of the indicated purified proteins. β(1,3)-Glucanosyl-transferase (*GT*) activities are in the *column on the right*. The activity was determined as described under "Experimental Procedures" and expressed as micromoles of rG13 consumed h^{-1}/mg of purified protein $\pm$ S.D. *N.d.*, activity not detectable.

Purified sGas1-Δ8Cys and sGas1-ΔL were also subjected to CD analysis (Fig. 6, *B* and *C*). The CD spectrum of sGas1-Δ8Cys showed that the protein still had a regular conformation with predominance of β-strand, but an increase in the β-turn content with respect to sGas1-ΔSer. Gas1-ΔL protein showed a remarkable change in the shape of the spectrum. Deconvolution of the profile indicated a high turn and random coil content suggesting that the deletion of the L region deeply affects the folding of the NtD.

From thermal denaturation curves obtained after monitoring ellipticity at the wavelength of 220 nm, the melting temperature (T_m) values of the truncated proteins were determined. The T_m for the truncated forms sGas1-ΔSer, sGas1-Δ8Cys, and sGas1-ΔL were 55.5, 52, and 51.2 °C, respectively, compared with the value of 56 °C of the full sGas1p previously reported (27). The kinetics of unfolding of sGas1-ΔL started at a temperature of about 10° centigrade lower than of the other proteins and was linear as expected from the loss of cooperative effects (data not shown). In conclusion the truncations of the 8Cys-box and the L region appear to negatively affect the stability of Gas1p.

The activity of the truncated proteins was first tested by an endo-β(1,3)glucanase assay using laminarin as a substrate, and the Gas mutants -Δ8Cys and -ΔL were found to be inactive (data not shown). Next we used a β(1,3)-glucanosyltransferase assay with a linear laminarioligosaccharide of 13 glucose residues (27). The results are summarized in the *right column* of Fig. 5. The activities of sGas1p and sGas1-ΔSer were similar, whereas sGas1-Δ8Cys and Gas1-ΔL were totally inactive (Fig. 5*A*, *right column*). The HPAEC profiles showed that the proteins were also inactive after a prolonged incubation time because products shorter or longer than the substrate, which are indicative of glucanosyltransferase activity, were not detected at 24 h of incubation (supplemental Fig. S4).

Next we asked whether the same behavior was exhibited by Gas2p. Two truncated versions, one lacking the GPI-attachment signal (sGas2) and one lacking also the 8Cys-box (sGas2-Δ8Cys), were expressed in *P. pastoris* (Fig. 5*B*). The purified proteins are shown in Fig. 5*C*. sGas2p and sGas2-Δ8Cys migrated as 62- and 45-kDa polypeptides, respectively. sGas2p
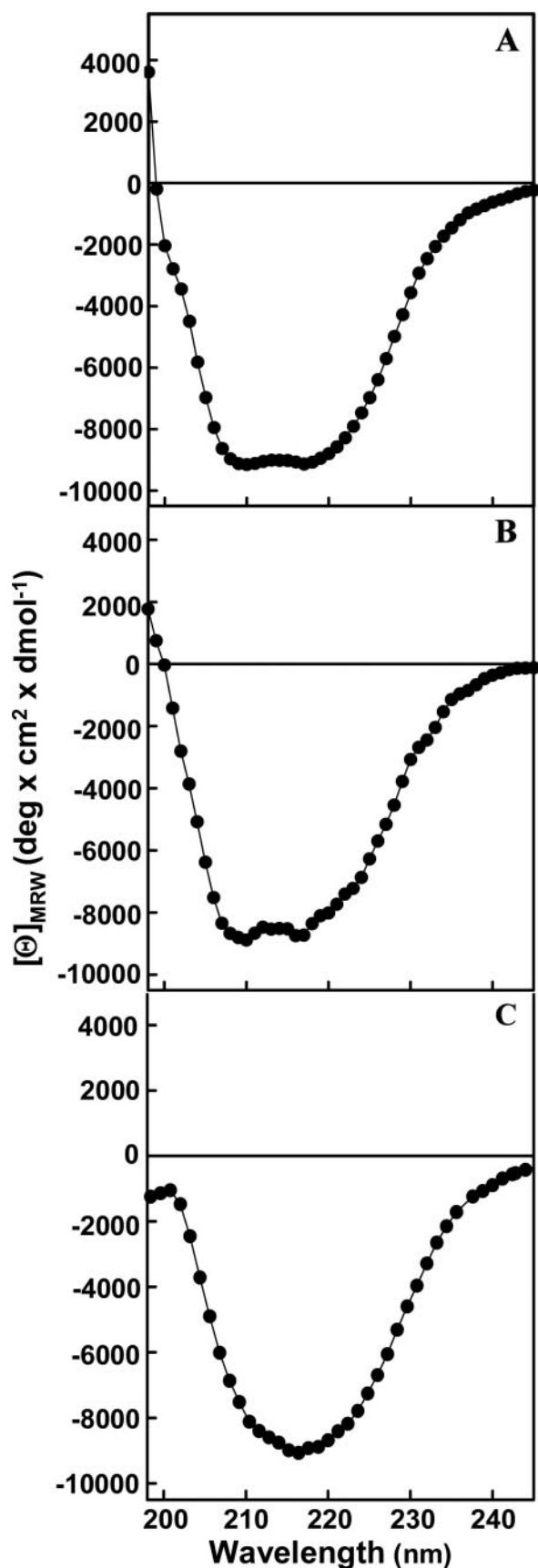
the truncated sGas1, ΔSer, Δ8Cys, and ΔL was 100, 90, 68, and 54 kDa, respectively. The proteins were both abundantly *N*- and *O*-glycosylated as expected from the presence of many potential *N*- and *O*-glycosylation sites.

To evaluate whether the truncations affect folding, purified proteins were subjected to CD analysis. sGas1p and sGas1-ΔSer showed quite similar far-UV CD spectra. Deconvolution data were indicative of a regular conformation with a predominance of β-strand in both proteins. The differential spectrum indicated that the Ser-rich region is in a random coil/β-turn conformation (supplemental Fig. S3). This is consistent with the predicted flexible role of this *O*-mannosylated stem that we demonstrated to be totally dispensable for the functionality of Gas1p (31). Because sGas1-ΔSer shares the same properties of sGas1p and the same activity, it will be used from here on as a reference protein.

FIGURE 6. **CD analysis of truncated proteins.** *A*, far-UV (200–250 nm) CD spectra of the indicated purified proteins at 20 °C. [*θ*]$_{MRW}$, means residue weight ellipticity. *A*, sGas1-ΔSer; *B*, sGas1-Δ8Cys; and *C*, sGas1-ΔL.

was expressed in the medium at a level comparable with sGas1p, whereas for sGas2-Δ8Cys the secretion level was lower (~0.5 mg/liter of medium at 48 h from induction). Although the mechanism for the decreased secretion of sGas2-Δ8Cys is not examined in this study, it is likely that the truncation affects the stability of the NtD + L region of Gas2p. In addition the 45-kDa polypeptide is not *N*-glycosylated, and this may contribute to its reduced secretion. Similarly to Gas1p, purified sGas2 showed *β*(1,3)-glucanosyltransferase activity, whereas sGas2-Δ8Cys was enzymatically inactive (*right column* Fig. 5*B*).

We attempted to express the 8Cys-box of Gas1p fused with the signal sequence of *PHO1* or *α*-factor in *P. pastoris*. The expression of the isolated 8Cys-box was never satisfactory (data not shown). The domain was expressed at a very low level (around 2 mg/liter) and was hyperglycosylated (data not shown). The abnormal glycosylation was because of an increased *N*-glycosylation at a unique *N*-glycosylation site (Asn^{490}–Gly–Ser^{492}) and to *O*-mannosylation. Target sites for glycosylation are likely to be masked in the full-length protein by the interaction between the 8Cys-box and the N-terminal domain, and they become accessible to the glycosylation machinery when the domain is expressed separately. Taken together this analysis indicates that neither the NtD nor the 8Cys-box is an independent domain of Gas1 or Gas2 proteins.

In conclusion our results demonstrate that the 8Cys-box is needed for the attainment of a stable conformation required for activity, whereas the L region plays a crucial role in the folding of the NtD domain. However, a full understanding of significance of these results must wait for the resolution of the three-dimensional structure of this enzyme.

Cys^{348} Is Essential for the Folding and Maturation of GPI-anchored Gas1p—To understand the importance of the conserved Cys residue located in the L region, Cys^{348} of Gas1p (corresponding to Cys^{367} in Gas2p) was replaced by a serine through site-directed mutagenesis. Gas1p and the mutant C348S were expressed in the original GPI-anchored form, and their expression was driven by the natural *GAS1* promoter. The construct was placed on a centromeric plasmid that was used to transform a *gas1*Δ mutant strain of *S. cerevisiae*. The cells expressing Gas1-C348S protein failed to complement the *gas1*Δ mutant phenotype as determined by the lack of suppression of the hypersensitivity to Calcofluor White, a cell wall perturbing agent that binds nascent chitin chains and interferes with the hyper-accumulation of chitin required for the viability of *gas1* cells (data not shown) (29). To determine whether the mutant protein was not functional or not properly produced, we performed a Western blot analysis. Previous studies by our lab and other laboratories demonstrated that Gas1p maturation along the secretory pathway is defined by an ER-form that migrates at 105 kDa and a mature form of 130 kDa produced after arrival at the Golgi (44–46). As shown in Fig. 7*A*, in total extracts from cells expressing Gas1p a major band of 130 kDa and a minor band of 105 kDa were detected, whereas in cells expressing the mutant Gas1p (C348S) only the reactive band at 105 kDa was detected suggesting either a block in maturation or secretion into the medium. To test this second hypothesis, medium proteins were precipitated and analyzed by Western blotting using anti-Gas1p antibodies. Gas1p and mutant Gas1p
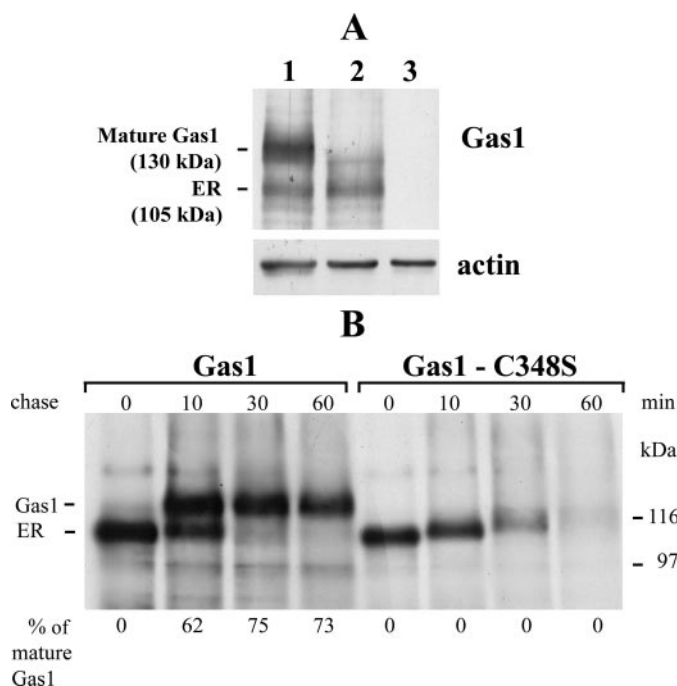
FIGURE 7. Cys[348] is essential for the maturation of the GPI-anchored form of Gas1p in *S. cerevisiae*. *A,* immunoblot with anti-Gas1 (*upper panel*) or anti-actin antibodies (*lower panel*) of total protein extracts (80 µg) from *gas1*Δ strain transformed with the YCplac33 vector harboring the *GAS1* gene (*lane 1*), the *GAS1*-C348S mutant gene (*lane 2*), or the empty vector (*lane 3*). A deliberately overexposed film is shown. The ER and mature forms of Gas1p are indicated. *B,* pulse labeling and immunoprecipitation with anti-Gas1p antibodies of cells harboring the YCplac33-*GAS1* plasmid or the YCplac33-*GAS1*-C348S plasmid. Cells were labeled for 7 min (time 0) and then chased for the indicated time points as described under "Experimental Procedures." The immunoprecipitates were subjected to SDS-PAGE. An overexposed autoradiogram of a representative gel shows the lack of maturation of the mutant protein. The immature (105 kDa) and mature (130 kDa) forms were quantified by densitometry analysis of an undersaturated film. *Below* each lane, the percentage of immature form converted into mature protein calculated in two separate experiments is shown. Consistent results were obtained from two different experiments.
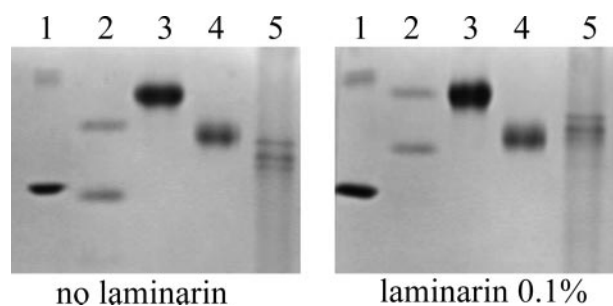

FIGURE 8. Qualitative affinity gel electrophoresis analysis of the interaction of sGas1p Ole e 10 and Ole e 9 with laminarin. BSA (*lane1*), Ole e 10 (*lane 2*), sGas1 (*lane 3*), sGas1-ΔSer (*lane 4*), and Ole e 9 (*lane 5*) were subjected to electrophoresis on native polyacrylamide gels in the absence or presence of laminarin. Proteins were stained with Coomassie Blue. Ole e 10 and Ole e 9 migrates as a doublet in these conditions.

folding of Gas1p and suggest that disposal of the misfolded C348S Gas1 protein occurs probably through ERAD (47). Interestingly, the radioactivity incorporated in the mutant Gas1 protein at the end of the pulse was ∼35% less than in Gas1p. This was a consequence of an equivalent 35% reduction in protein synthesis as measured by incorporation of radioactivity in the cold trichloroacetic acid-precipitable material from cell cultures at the end of the 7-min pulse. This reduction in protein synthesis suggests a global attenuation of protein synthesis as occurs when the unfolded protein response is triggered (48, 49). These results point to an essential role of Cys[348] in the folding of Gas1p.

Comparison of the Polysaccharide Binding Properties of sGas1 and Olive Pollen Allergens Ole e 9 and Ole e 10—In plants, the Cys-box (X8 domain) is present in one or more copies and is often appended to a catalytic domain as in the group of "long" GH17 $\beta(1,3)$-glucanases or exists as a small lectin-like polypeptide (Fig. 1*B*). Because Ole e 10 was shown to have a high affinity for laminarin (41), a mixture of soluble $\beta(1,3)$-glucans with an average degree of polymerization of 25 glucose residues, the X8 domain was also annotated in family 43 of carbohydrate-binding module of the CAZy data base (carbohydrate-binding module 43). However, no detailed analysis has so far been performed on fungal enzymes. Therefore, we analyzed the properties of binding to $\beta(1,3)$-glucan of Gas1p in comparison with Ole e 9 and Ole e 10. We set up AGE analysis that was previously used to assess the high affinity binding of Ole e 10 to laminarin (41). The interaction of these proteins with the soluble polysaccharide was revealed by the retardation of the electrophoretic mobility in a native gel polymerized in the presence of the polysaccharide with respect to a gel that does not contain it (32, 50). As shown in Fig. 8, sGas1 and sGas1-ΔSer did not show any shift in electrophoretic mobility in a native gel containing laminarin (*lanes 3 and 4*), whereas the Ole e 10 and Ole e 9 proteins were retarded (*lanes 2 and 5*), and the mobility of BSA, used as a negative control, was not influenced (*lane 1*). The Ole e 10-laminarin complex was previously reported to have a K_d of 290 µM (K_a of 3.4×10^3 M^{-1}) (41). Because AGE is sensitive to an interaction association constant (K_a) ranging from ∼10^2 to 10^5 M^{-1} that are typical of lectins, we can conclude that sGas1p affinity for laminarin is not in this range, and the protein does not possess lectin-like property toward laminarin. A similar behavior upon AGE was observed for sGas2p (data not shown). The high K_m value determined for the $\beta(1,3)$-

were not detected in the medium of cells during vegetative growth (data not shown). Then, to test more accurately the effect of C348S replacement on Gas1p biosynthesis, we performed pulse-chase experiments. Cells were labeled for 7 min with radioactive methionine and cysteine, and the fate of the labeled precursor was monitored at different time points of chase. At the end of the chase Gas1p migrated at 105 kDa (Fig. 7*B*). At 10 min chase about 62% of Gas1p was converted to the mature form. At 30 and 60 min only the mature Gas1p was detected indicating an efficient maturation of the precursor. At the end of the pulse mutant Gas1p also migrated at 105 kDa but at 10 min of chase only a slight upward shift was detected, and the immature polypeptide migrated at about 110 kDa (Fig. 7*B*). At 30 min of chase the labeling was fainter and diffuse, and the mutant protein migrated at about 115 kDa suggesting a further increase in size and heterogeneity. At 60 min of chase only a very diffuse and faint band was detected. At each time point the 130-kDa band was not present. Therefore, the C348S substitution results in a 105-kDa ER form unable to reach the Golgi and progressively degraded after having acquired some type of modifications that slightly increase its molecular mass. Taken together, these results point to an essential role of Cys[348] in the

glucanosyltransferase reaction of a GH72 enzyme (5) is compatible with these results.

In another set of experiments, we used an alkali-insoluble fraction of the cell wall, which is enriched in $\beta(1,3)$-glucan, to evaluate the capability of binding of sGas1p. Gas1p did not show any specific binding (data not shown) suggesting that the 8Cys-box does not confer a lectin-like behavior toward either soluble or insoluble $\beta(1,3)$-glucan.

DISCUSSION

We have reported here the successful application of a combined strategy, based on advanced mass spectrometric analysis and appropriate conditions of protein cleavage, for the determination of intramolecular disulfide bonds of extracellular glycoproteins. Mapping of disulfide bonds in proteins requires cleavage between Cys residues. We used chemical cleavage at Asp at pH 2 at elevated temperature, combined with enzymatic cleavage at the C-terminal peptide bonds of Glu residues by endoproteinase Glu-C. Disulfide-linked proteins are often resistant to protease digestion, requiring chemical cleavage. Cleavage at Asp is convenient because of the ubiquity of this amino acid and the simplicity of the reaction, but it is only partial under the experimental conditions. Partial cleavage results in complex peptide mixtures containing ensembles of peptides with a particular disulfide bond. We show here that a complicated disulfide bond network of a 60-kDa protein can be unraveled with a single LC/MS run with a few picomoles of a protein digest using a high mass accuracy FTICR mass spectrometer, provided that cleavage can be achieved between consecutive Cys residues to yield peptides with a single disulfide bond. The structure of peptides with two disulfide bonds was solved by partial reduction of disulfide bonds, followed by cyanylation of partial reduction products and ammonia-induced cleavage of the peptides at cyanylated Cys residues. This series of reactions was carried out in one reaction vial without sample clean up between the different steps and directly followed by LC/MS analysis. We used HPLC to obtain fractions enriched in peptides with two disulfide bonds, but it might also be feasible to apply this approach on whole protein digests. This will save time and material. Identifying cleavage products by mass spectrometry may be facilitated by cleavage in both ammonia and in the presence of methylamine in parallel reactions, as products with a defined mass difference, *i.e.* 14 Da, are formed under these conditions (51).

This analytical method was applied to the characterization of the disulfide bridges in Gas1 and Gas2 proteins. The 14 conserved Cys residues that Gas1p and Gas2p share with all the known members of family GH72$^+$ form seven disulfide bridges. These bonds connect distant parts of the protein, and their characterization provided insight into the structure of the Gas proteins. Two separate intra-domain networks of disulfide bonds were identified. A first nucleus includes three disulfide bonds, one of which could not be predicted by molecular modeling (40). This extra bond connects the conserved Cys residue located in the L region with one central Cys residue of the NtD (Cys^{216}–Cys^{348} in Gas1p and Cys^{231}–Cys^{367} in Gas2). The NtD, spanning residues 23–332 of Gas1p and 23–346 in Gas2p, is predicted to assume a TIM barrel fold with the N terminus

close to the C terminus (40). Therefore, the bond we have identified supports a role of the L region as an extra tail of the TIM barrel that stabilizes the NtD. Furthermore, the L region could bring the 8Cys-box into close proximity with the NtD. The identification of the disulfide bonds and the distance constraints provided by the disulfide bonds will allow a refinement of the proposed molecular model (40).

The four remaining disulfide bonds are all within the 8Cys-box. Interestingly, we have identified an extra bond in the yeast Cys-box compared with the plant Cys-box/X8 domain (Fig. 3). Secondary structure predictions suggest the existence of relevant differences between the yeast 8Cys-box and the plant 6Cys-box. Functional analysis indicate that truncation of the 8Cys-box abolishes the glucanosyltransferase activity of Gas1 and Gas2 proteins. We propose that the 8Cys-box could (i) contribute to the substrate binding together with the NtD, (ii) induce a conformational change required for the activity, or (iii) play a role in the folding of the NtD + L portion. A more definite interpretation of these results will rely on the availability of the crystal structure of these enzymes and on further studies.

Taken together our results suggest a close interaction of NtD with the 8Cys-box. This behavior differs greatly from that reported for Ole e 9. In the plant enzyme, the N- and C-terminal domains are structurally and functionally independent and can be separately produced at high expression levels by recombinant DNA technology. Each recombinant domain retains its properties; the N-terminal domain is catalytically active, and the C-terminal domain functions as a module of high affinity binding to $\beta(1,3)$-glucan (52, 53). It is likely that this module is the only means for targeting the pollen enzyme at sites where hydrolysis of callose and $1,3:1,4$-β-glucan takes place during pollen tube elongation (41).

Secretory proteins are generally rich in disulfide bonds. Disulfide bonds promote long term protein stability for folded conformations, and their formation is an essential step in the folding process of many secretory proteins. We have shown that the mutant Gas1-C348S is entrapped in a folding intermediate that is no longer processed to the mature form. Therefore, the Cys^{348} located in the L region is a crucial residue for the proper folding of Gas1 protein. A similar behavior was previously shown for Cys^{74} that is also crucial for the folding process of Gas1p (27). The unprocessed intermediates are probably substrates for ERAD that could target the misfolded Gas1 protein to ubiquitination and degradation in the cytoplasm (47). It has been recently shown that *O*-mannosylation is required for detection and subsequent degradation of a misfolded form of Gas1p by the proteasome (54).

It is still an open question why some fungal $\beta(1,3)$-glucanosyltransferases lack the Cys-box despite exhibiting a similar activity. We have recently shown that Gas1p and Gas2 share an identical preference for cleavage sites, whereas Gas3, Gas4, and Gas5, which belong to GH72$^-$, showed different preferences for cleavage sites in an *in vitro* assay (17). It is not yet known whether these enzymes act solely on newly synthesized $\beta(1,3)$-glucan or also have a role in the remodeling of the existing $\beta(1,3)$-glucan network during cell growth or adaptation to a changing environment. It was also never examined whether they require a relaxed or extended conformation of the sub-

strate that is known to be endowed of elastic properties *in vivo* (3, 4). Different GH72$^+$ and GH72$^-$ enzymes could satisfy the cellular needs to remodel β(1,3)-glucan in different physiological conditions and in different conformations. In this regard it is interesting to note that the plant xylanoglucan endotransferase XET, a key enzyme that first cleaves and then religates xyloglucan polymers in plant cell walls, requires a C-terminal extension that may modulate the catalytic mechanism of XET family of proteins (55). A similar situation can be envisaged for GH72 enzymes that harbor different C-terminal extensions and could have different specificities for different types of β(1,3)-glucan conformations. This could provide an explanation to the redundancy of the GH72 enzymes.

REFERENCES

1. Lesage, G., and Bussey, H. (2006) *Microbiol. Mol. Biol. Rev.* **70,** 317–343
2. Klis, F. M., Boorsma, A., and De Groot, P. W. (2006) *Yeast* **23,** 185–202
3. Rees, D. A., and Scott, W. E. (1971) *J. Chem. Soc.* (*Lond.*) (B) **1971,** 469–479
4. Rees, D. A., Morris, E. R., Thom, D., and Madden, J. K. (1982) in *The Polysaccharides* (Aspinall, G. O. E., ed) Vol. I, pp. 196–290, Academic Press, New York
5. Hartland, R. P., Fontaine, T., Debeaupuis, J. P., Simenel, C., Delepierre, M., and Latge, J. P. (1996) *J. Biol. Chem.* **271,** 26843–26849
6. Mouyna, I., Monod, M., Fontaine, T., Henrissat, B., Lechenne, B., and Latge, J. P. (2000) *Biochem. J.* **347,** 741–747
7. Popolo, L., Vai, M., Gatti, E., Porello, S., Bonfante, P., Balestrini, R., and Alberghina, L. (1993) *J. Bacteriol.* **175,** 1879–1885
8. Popolo, L., Gualtieri, T., and Ragni, E. (2001) *Med. Mycol.* **39,** 111–121
9. Popolo, L., Gilardelli, D., Bonfante, P., and Vai, M. (1997) *J. Bacteriol.* **179,** 463–469
10. Popolo, L., and Vai, M. (1999) *Biochim. Biophys. Acta* **1426,** 385–400
11. Lesage, G., Sdicu, A. M., Menard, P., Shapiro, J., Hussein, S., and Bussey, H. (2004) *Genetics* **167,** 35–49
12. Lagorce, A., Hauser, N. C., Labourdette, D., Rodriguez, C., Martin-Yken, H., Arroyo, J., Hoheisel, J. D., and Francois, J. (2003) *J. Biol. Chem.* **278,** 20345–20357
13. Ragni, E., Coluccio, A., Rolli, E., Rodriguez-Pena, J. M., Colasante, G., Arroyo, J., Neiman, A. M., and Popolo, L. (2007) *Eukaryot. Cell* **6,** 302–316
14. de Medina-Redondo, M., Arnaiz-Pita, Y., Fontaine, T., Del Rey, F., Latge, J. P., and Vazquez de Aldana, C. R. (2008) *Mol. Microbiol.* **68,** 1283–1299
15. Mouyna, I., Morelle, W., Vai, M., Monod, M., Lechenne, B., Fontaine, T., Beauvais, A., Sarfati, J., Prevost, M. C., Henry, C., and Latge, J. P. (2005) *Mol. Microbiol.* **56,** 1675–1688
16. De Bernardis, F., Muhlschlegel, F. A., Cassone, A., and Fonzi, W. A. (1998) *Infect. Immun.* **66,** 3317–3325
17. Ragni, E., Fontaine, T., Gissi, C., Latge, J. P., and Popolo, L. (2007) *Yeast* **24,** 297–308
18. Yin, Q. Y., de Groot, P. W., de Jong, L., Klis, F. M., and De Koster, C. G. (2007) *FEMS Yeast Res.* **7,** 887–896
19. Yin, Q. Y., de Groot, P. W., Dekker, H. L., de Jong, L., Klis, F. M., and de Koster, C. G. (2005) *J. Biol. Chem.* **280,** 20894–20901
20. Sunna, A., Gibbs, M. D., and Bergquist, P. L. (2001) *Biochem. J.* **356,** 791–798
21. Boraston, A. B., Bolam, D. N., Gilbert, H. J., and Davies, G. J. (2004) *Biochem. J.* **382,** 769–781
22. de Koning, L. J., Kasper, P. T., Back, J. W., Nessen, M. A., Vanrobaeys, F., Van Beeumen, J., Gherardi, E., de Koster, C. G., and de Jong, L. (2006) *FEBS J.* **273,** 281–291
23. Inglis, A. S. (1983) *Methods Enzymol.* **91,** 324–332
24. Wu, J., and Watson, J. T. (1997) *Protein Sci.* **6,** 391–398
25. Nakagawa, S., Tamakashi, Y., Hamana, T., Kawase, M., Taketomi, S., Ishibashi, Y., Nishimura, O., and Fukada, T. (1994) *J. Am. Chem. Soc.* **116,** 5513–5514
26. Wu, J., and Watson, J. T. (2002) *Methods Mol. Biol.* **194,** 1–22
27. Carotti, C., Ragni, E., Palomares, O., Fontaine, T., Tedeschi, G., Rodriguez, R., Latge, J. P., Vai, M., and Popolo, L. (2004) *Eur. J. Biochem.* **271,** 3635–3645
28. Vai, M., Gatti, E., Lacana, E., Popolo, L., and Alberghina, L. (1991) *J. Biol. Chem.* **266,** 12242–12248
29. Valdivieso, M. H., Ferrario, L., Vai, M., Duran, A., and Popolo, L. (2000) *J. Bacteriol.* **182,** 4752–4757
30. Ozols, J. (1990) *Methods Enzymol.* **182,** 587–601
31. Gatti, E., Popolo, L., Vai, M., Rota, N., and Alberghina, L. (1994) *J. Biol. Chem.* **269,** 19695–19700
32. Tomme, P., Boraston, A., Kormos, J. M., Warren, R. A., and Kilburn, D. G. (2000) *Enzyme Microb. Technol.* **27,** 453–458
33. Boone, C., Sommer, S. S., Hensel, A., and Bussey, H. (1990) *J. Cell Biol.* **110,** 1833–1843
34. Perczel, A., Hollosi, M., Tusnady, G., and Fasman, G. D. (1991) *Protein Eng.* **4,** 669–679
35. Finn, R. D., Mistry, J., Schuster-Bockler, B., Griffiths-Jones, S., Hollich, V., Lassmann, T., Moxon, S., Marshall, M., Khanna, A., Durbin, R., Eddy, S. R., Sonnhammer, E. L., and Bateman, A. (2006) *Nucleic Acids Res.* **34,** D247–D251
36. Jones, D. T. (1999) *J. Mol. Biol.* **292,** 195–202
37. Bryson, K., McGuffin, L. J., Marsden, R. L., Ward, J. J., Sodhi, J. S., and Jones, D. T. (2005) *Nucleic Acids Res.* **33,** W36–W38
38. Cuff, J. A., and Barton, G. J. (2000) *Proteins* **40,** 502–511
39. Fonzi, W. A. (1999) *J. Bacteriol.* **181,** 7070–7079
40. Papaleo, E., Fantucci, P., Vai, M., and De Gioia, L. (2006) *J. Mol. Model* **12,** 237–248
41. Barral, P., Suarez, C., Batanero, E., Alfonso, C., Alche Jde, D., Rodriguez-Garcia, M. I., Villalba, M., Rivas, G., and Rodriguez, R. (2005) *Biochem. J.* **390,** 77–84
42. Huecas, S., Villalba, M., and Rodriguez, R. (2001) *J. Biol. Chem.* **276,** 27959–27966
43. Trevino, M. A., Palomares, O., Castrillo, I., Villalba, M., Rodriguez, R., Rico, M., Santoro, J., and Bruix, M. (2008) *Protein Sci.* **17,** 371–376
44. Schimmoller, F., Singer-Kruger, B., Schroder, S., Kruger, U., Barlowe, C., and Riezman, H. (1995) *EMBO J.* **14,** 1329–1339
45. Vai, M., Popolo, L., Grandori, R., Lacana, E., and Alberghina, L. (1990) *Biochim. Biophys. Acta* **1038,** 277–285
46. Frand, A. R., and Kaiser, C. A. (1998) *Mol. Cell* **1,** 161–170
47. Meusser, B., Hirsch, C., Jarosch, E., and Sommer, T. (2005) *Nat. Cell Biol.* **7,** 766–772
48. Kaufman, R. J. (2004) *Trends Biochem. Sci.* **29,** 152–158
49. Zhang, K., and Kaufman, R. J. (2004) *J. Biol. Chem.* **279,** 25935–25938
50. Hong, T. Y., Cheng, C. W., Huang, J. W., and Meng, M. (2002) *Microbiology* **148,** 1151–1159
51. Gallegos-Perez, J. L., Rangel-Ordonez, L., Bowman, S. R., Ngowe, C. O., and Watson, J. T. (2005) *Anal. Biochem.* **346,** 311–319
52. Palomares, O., Villalba, M., Quiralte, J., Polo, F., and Rodriguez, R. (2005) *Clin. Exp. Allergy* **35,** 345–351
53. Palomares, O., Villalba, M., and Rodriguez, R. (2003) *Biochem. J.* **369,** 593–601
54. Hirayama, H., Fujiita, M., Yoko-O, T., and Jigami, Y. (2008) *J. Biochem.* (*Tokyo*) **143,** 555–567
55. Johansson, P., Brumer, H., 3rd, Baumann, M. J., Kallas, A. M., Henriksson, H., Denman, S. E., Teeri, T. T., and Jones, T. A. (2004) *Plant Cell* **16,** 874–886